IC/83/150

INTERNATIONAL CENTRE FOR THEORETICAL PHYSICS

THEORY OF THE INTERFACE BETWEEN A CLASSICAL PLASMA AND A HARD WALL

P. Ballone

G. Pastore

and

M.P. Tosi

INTERNATIONAL ATOMIC ENERGY AGENCY

UNITED NATIONS EDUCATIONAL, SCIENTIFIC AND CULTURAL ORGANIZATION

1983 MIRAMARE-TRIESTE

IC/83/150

International Atomic Energy Agency
and
United Nations Educational Scientific and Cultural Organization

INTERNATIONAL CENTRE FOR THEORETICAL PHYSICS

THEORY OF THE INTERFACE BETWEEN A CLASSICAL PLASMA AND A HARD WALL *

P. Ballone and G. Pastore
International School for Advanced Studies, Trieste, Italy,

and

M.P. Tosi
International Centre for Theoretical Physics, Trieste, Italy
and
Istituto di Fisica Teorica, Università di Trieste, Italy.

MIRAMARE - TRIESTE
September 1983

* Submitted for publication.

Abstract. The interfacial density profile of a classical one-component plasma confined by a hard wall is studied in planar and spherical geometries. The approach adapts to interfacial problems a modified hypernetted-chain approximation developed by Lado and by Rosenfeld and Ashcroft for the bulk structure of simple liquids. The specific new aim is to embody selfconsistently into the theory a 'contact theorem', fixing the plasma density at the wall through an equilibrium condition which involves the electrical potential drop across the interface and the bulk pressure. The theory is brought into fully quantitative contact with computer simulation data for a plasma confined in a spherical cavity of large but finite radius. It is also shown that the interfacial potential at the point of zero charge is accurately reproduced by suitably combining the contact theorem with relevant bulk properties in a simple, approximate representation of the interfacial charge density profile.

1. Introduction

The interface between a liquid electrolyte and a metallic electrode has been a subject of great theoretical and practical interest for a long time.[1] The simplest model that may be helpful to clarify some of the statistical-mechanical aspects of the theory of such an interface is provided by a classical one-component plasma confined by a planar hard wall with no image forces.

Computer simulation data have recently been reported[2] for this model interface, although for convenience the plasma was confined in a spherical cavity of large but finite radius R. These data on the interfacial charge density profile are only qualitatively reproduced by statistical-mechanical theories of the planar interface, based on the mean spherical approximation (MSA) or on the hypernetted chain approximation (HNC).

Concentrating on the strong coupling regime where the interfacial density profile shows pronounced layering of the plasma near the wall, it is useful to recall the well-known analogy between a planar confining wall and a hard impurity of radius tending to infinity. This analogy suggests that the amplitude and the phase of the density oscillations are largely determined by conditions obtaining near contact with the wall, whereas their wavelength and decay rate are, at least asymptotically, determined by bulk properties.[3] Similar considerations apply in the weak coupling regime, where the decay of the profile is monotonic.

A 'contact theorem' for electrolytes confined by a hard wall, relating the particle densities at contact to electrical and thermodynamic quantities through an exact pressure balance condition, has been demonstrated by Henderson *et al*[4] and extended to plasmas on a neutralizing background by Totsuji.[5,6] This balance condition is incorporated selfconsistently into the theory of the wall-plasma

interface in this paper, through a suitable adaptation of a modified-HNC approximation (MHNC) previously developed by Lado[7] and by Rosenfeld and Ashcroft[8] for the bulk structure of simple liquids, including the one-component plasma.

The theory and the numerical results for the case of a planar confining wall are presented in sections 2 and 3 of the paper. An appreciable strengthening of the local layering of the plasma near the wall, in accord with the computer simulation data, and a greatly improved account of the potential at the point of zero charge are the main results of these calculations relative to the previous MSA and HNC theories. In order to establish fuller contact with the simulation work, the case of a plasma in contact with a curved wall is then considered in section 4. Although the spherical simulation box has a reasonably large radius ($R = (6.9 \div 8.8)a$, where $a = (4\pi n/3)^{-1/3}$ in terms of the average particle density n), finiteness effects are still quantitatively relevant in further strengthening the local layering of the plasma. A brief summary and discussion are finally given in section 5 of the paper.

2. Planar interface: theory

In brief, the present MHNC approach introduces approximate bridge function contributions to the wall-plasma correlation function (i.e. the interfacial density profile) and to the plasma pair correlation function. The bridge functions are taken from the Percus-Yevick theory of hard-sphere fluids and are empirically adjusted to account for the contact theorem in the interface and for thermodynamic consistency in the bulk. Whereas an approximately universal behaviour of the bridge function could be demonstrated[8] for bulk one-component fluids on the basis of computer simulation

data, the evidence on interfaces does not allow as yet a precise test of a similar universality hypothesis. No counter-indication has emerged, however, from our preliminary analysis of available simulation data on systems with different force laws.[2,9]

2.1 Bulk structure

Starting from the bulk plasma correlations, that we shall need later, the bridge function b(r) is defined by writing the radial distribution function g(r) in the form

$$g(r) = \exp\left[-\beta\phi(r) + h(r) - c(r) - b(r)\right] \qquad (2.1)$$

where $\beta = (k_B T)^{-1}$, $\phi(r) = e^2/r$, $h(r) = g(r) - 1$, and c(r) is the direct correlation function entering the Ornstein-Zernike integral equation,

$$h(r) = c(r) + n\int d\underline{r}'\, c(|\underline{r}-\underline{r}'|)h(r'). \qquad (2.2)$$

The assumption $b(r) = 0$ yields the HNC closure of the hierarchy, allowing a solution of eqns (2.1) and (2.2) for g(r) and c(r).

Following Rosenfeld and Ashcroft,[8] we replace b(r) in eqn (2.1) by its value in the Percus-Yevick theory for a fluid of neutral hard spheres ($b_{PY}(r)$, say). The function $b_{PY}(r)$ represents a family of essentially short-ranged curves which depend only on the packing fraction η as a parameter, the appropriate value of this parameter being fixed by imposing thermodynamic consistency on the isothermal compressibility K_T. More precisely, we determine η from the condition

$$K_0/K_T = 1 - n\int d\underline{r}\left[c(r) + \beta e^2/r\right] \qquad (2.3)$$

where K_0 is the ideal gas compressibility and K_T is known from simulation data[10] as a function of the plasma coupling parameter $\Gamma = \beta e^2/a$. This approach yields values for g(r) in the one-component plasma which agree within about 1% with computer simulation data reported by Hansen.[11]

2.2 Wall-plasma correlations

We start now from the Ornstein-Zernike integral equations for a two-component fluid, component 1 being the plasma particles and component 2 a system of hard spheres of density n_2 and diameter σ_2. The limit of a plsma confined by a planar hard wall is obtained[12] by letting $n_2 \to 0$ and $\sigma_2 \to \infty$ with $n_2\sigma_2^3 \to 0$. The Ornstein-Zernike equation for the 1-2 correlations becomes in this limit

$$h_{12}(r) = c_{12}(r) + n\int d\underline{r}' c_{11}(|\underline{r}-\underline{r}'|)h_{12}(r') \qquad (2.4)$$

where $c_{11}(r)$ is the bulk plasma direct correlation function, already discussed in section 2.1 above. Setting $r = \frac{1}{2}\sigma_2 + z$, with $z = 0$ on the wall, $h_{12}(r)$ in eqn (2.4) determines the interfacial density profile $n(z)$ through

$$h_{12}(r) \to n(z)/n - 1. \qquad (2.5)$$

We next supplement eqn (2.4) with the MHNC closure for the wall-plasma correlations. The corresponding bridge function $b_{12}(r)$ is introduced by writing

$$g_{12}(r) = \exp\left[-\beta\phi_{12}(r) + h_{12}(r) - c_{12}(r) - b_{12}(r)\right], \qquad (2.6)$$

where $\phi_{12}(r)$ is the bare interaction potential between the wall and the plasma particles, given by $\phi_{12}(z) = \infty$ for $z < 0$ and by $\phi_{12}(z) = 0$ for $z > 0$ in the present case of an uncharged hard wall without image forces. The function $b_{12}(r)$ in eqn (2.6) is approximated, in the limit mentioned above, by $b_{12}^{PY}(z)$ from the Percus-Yevick theory for a fluid of neutral hard spheres confined by a hard wall. This gives

$$b_{12}^{PY}(z) = \begin{cases} -c_{12}^{PY}(z) - 1 - \ln\left[-c_{12}^{PY}(z)\right] & \text{for } -\frac{1}{2}\sigma < z < \frac{1}{2}\sigma \\ h_{12}^{PY}(z) - \ln\left[1 + h_{12}^{PY}(z)\right] & \text{for } z > \frac{1}{2}\sigma \end{cases} \qquad (2.7)$$

where σ is the hard sphere diameter and the functions $c_{12}^{PY}(z)$ and $h_{12}^{PY}(z)$ are known from the analytic solution[13] of the Percus-Yevick theory for a two-component mixture of hard spheres. The packing fraction $\eta' = \frac{\pi}{6}n\sigma^3$ entering $b_{12}^{PY}(z)$ will be determined in the calculations reported below from the contact theorem for the plasma[5],

$$k_B T n(0) = p - ne\Delta\varphi \ , \qquad (2.8)$$

$p = -(\partial F/\partial V)_T$ being the pressure in the bulk plasma at given coupling strength Γ and $\Delta\varphi = \varphi(0) - \varphi(\infty)$ being the electrical potential drop between the wall and the bulk plasma.

The final step consists in taking explicit account, as usual, of the singular Coulomb term $-\beta e^2/r$ entering $c_{11}(r)$ in eqn (2.4). After some simple algebra, eqn (2.4) can be written in the form

$$n(z)/n = 1 + c_{12}(z) - \beta e\varphi(z) + \Psi(z) \qquad (2.9)$$

where $\Psi(z)$ is defined by

$$\Psi(z) \equiv 2\pi n\int_{-\infty}^{\infty} dz'\left[\frac{n(z')}{n} - 1\right]\int_{|z-z'|}^{|z+z'|} dr\left[rc_{11}(r) + \beta e^2\right] \qquad (2.10)$$

and $\varphi(z)$ is the electrostatic (Hartree) potential, determined self-consistently through the Poisson equation

$$\frac{d^2\varphi(z)}{dz^2} = -4\pi e\left[n(z) - n\right] . \qquad (2.11)$$

Equations (2.9)-(2.11) are combined with the MHNC closure, i.e.

$$\ln\left[n(z)/n\right] = -\beta\phi_{12}(z) + \frac{n(z)}{n} - 1 - c_{12}(z) - b_{12}^{PY}(z) \qquad (2.12)$$

with $b_{12}^{PY}(z)$ given by eqn (2.7). Clearly, $c_{12}(z)$ can be eliminated by combining eqns (2.9) and (2.12) to yield the density profile equation as

$$\ln\left[n(z)/n\right] = -\beta e\varphi(z) + \Psi(z) - b_{12}^{PY}(z) \qquad (z > 0) \ . \qquad (2.13)$$

This equation is solved selfconsistently with the Poisson equation, the input being the bulk plasma correlation function $c_{11}(r)$, evaluated as discussed in section 2.1, and the function $b_{12}^{PY}(z)$, selfconsistently adjusted to satisfy the contact theorem (2.8).

3. Planar interface: numerical results

The numerical calculations of the interfacial density profile have been carried out by the method used by Badiali *et al*[2]. If we set $b_{12}(z) = 0$ but keep $b(r) = b_{PY}(r)$ in eqn (2.1), we essentially reproduce the results that they obtained by treating the wall-plasma correlations in the HNC and by using Monte Carlo data for bulk correlations (HNC/MC scheme). These results will be compared below with those of the full MHNC/MHNC approach.

Before we do this, it is interesting to compare in Figure 1 the bridge functions for the bulk and for the interface, over a relevant range of values of the effective packing fraction. Clearly, this correction to the HNC is appreciably more localised near the flat wall than in the bulk radial distribution function.

The results for the density profile at $\Gamma = 30$ are reported in Figure 2, this being illustrative of the results that we have obtained also for other values of the coupling strength. The inclusion of interfacial bridge graphs is modifying appreciably the calculated profile, in the direction indicated by the simulation data. The simulation value of the contact density n(0) is rather well reproduced in the MHNC/MHNC, whereas there remain discrepancies in the amplitude of the profile oscillations and also in their phase. We shall enquire about the origin of these discrepancies in the next section, where we shall examine the effects of enclosing the plasma in a spherical box as was done in the simulation work.

Additional illustration of the effect of satisfying the contact theorem is given in Table 1. This reports the values of n(0) and of the total potential drop $\Delta\varphi$ as calculated in the MHNC/MHNC, as well as in the HNC/MC and MSA/MSA schemes explored by Badiali *et al*[2], against the Monte Carlo (MC) simulation data.

The last column for each entry in Table 1 shows the results of a very simple calculation, using only the asymptotic form of

the density profile, which are given[3] by

$$n(z) = n + a_1 \exp(-\lambda_1 z) + a_2 \exp(-\lambda_2 z) \qquad (3.1)$$

at weak coupling ($\Gamma \lesssim 2.8$) and by

$$n(z) = n + A\exp(-\lambda_1 z)\cos(\lambda_2 z + \vartheta) \qquad (3.2)$$

at strong coupling ($\Gamma \gtrsim 2.8$). The quantities λ_1 and λ_2 are determined from bulk properties[3] calculated in the MHNC, and the quantities a_1 and a_2 (or A and ϑ) are determined by imposing overall charge neutrality and the contact theorem (2.8). For example, from eqn (3.2) we find almost immediately

$$n(0)/n = 1 + \frac{\lambda_1^2 + \lambda_2^2}{\lambda_1^2 + \lambda_2^2 + k_D^2} \frac{U}{3k_BT} \qquad (3.3)$$

and

$$\Delta\varphi = 4\pi e \frac{n(0) - n}{\lambda_1^2 + \lambda_2^2} , \qquad (3.4)$$

U being the mean potential energy per particle in the bulk plasma and k_D the inverse Debye screening length. The excellent results obtained in this way for n(0) and $\Delta\varphi$ stress the practical importance of the contact theorem at strong couplings, where the profile of the electrical potential consists of a sharp drop followed by extended oscillations so that the total potential drop is crucially influenced by conditions in the immediate neighbourhood of the wall.

As a last remark, we note that the above simple approach can be easily extended to the case of a charged wall, yielding a simple estimate of the differential capacitance of the interface as a function of the surface charge density. Unfortunately, no simulation results are as yet available on this property. The capacitance at the point of zero charge increases continuously with increasing Γ, a rather dull behaviour when contrasted with the observed temperature dependence of this quantity for metal-molten salt interfaces[14].

4. Plasma in large spherical cavity

Turning now to a neutralized plasma in a spherical cavity of large radius R, we start from the equation for the density profile n(r) in the form

$$\ln\left[n(r)/n\right] = \int d\underline{r}'\, c_{11}(|\underline{r}-\underline{r}'|)\left[n(r') - n\right] - b_{12}(r) \quad , \qquad (4.1)$$

for $0 \leq r < R$. After separating out the singular Coulomb part of $c_{11}(r)$, we can write the analogue of eqn (2.13) as

$$\ln\left[n(r)/n\right] = -\beta e\varphi(r) + \Psi(r) - b_{12}(r) \qquad (0 \leq r < R) \qquad (4.2)$$

where $\Psi(r)$ is defined by

$$\Psi(r) \equiv \frac{2\pi n}{r}\int_0^\infty sds\left[\frac{n(s)}{n} - 1\right]\int_{|r-s|}^{r+s} du\left[uc_{11}(u) + \beta e^2\right] \qquad (4.3)$$

and $\varphi(r)$ is the solution of Poisson's equation

$$\frac{d^2\varphi(r)}{dr^2} + \frac{2}{r}\frac{d\varphi(r)}{dr} = -4\pi e\left[n(r) - n\right]. \qquad (4.4)$$

Here, $c_{11}(r)$ is again taken as the direct correlation function in the bulk plasma, and the bridge function $b_{12}(r)$ remains to be determined. The method of integration of the Poisson equation followed[2] in the case of a planar wall is easily adapted to the present case.

The modifications induced in $b_{12}^{PY}(z)$ and in the contact theorem by the curvature of the interface are not known. For a first calculation we have taken these forms from the case of the planar wall and the results are shown in Figures 3-5 for values of Γ in the oscillatory-profile regime, the values of R being chosen to be those of the simulation work. There are appreciable modifications of the profile relative to the case of the planar wall, as can be seen from the Figures, these modifications being mainly due to the fact that one is now solving Poisson's equation in spherical geometry rather than in planar geometry.

Since the contact value of the density is again rather well reproduced by the above calculations, the main correction for the discrepancies that still remain between theory and simulation may be subsumed in the form of the interfacial bridge function. Recalling the results of Figure 1 for the bulk and interfacial bridge functions, we have tried a simple scaling down of the width of $b_{12}^{PY}(z)$ to adapt it to the case of the curved interface. This allows a successful fit of the simulation data, as is shown in Figures 3-5. The corresponding values of the contact density and the potential drop are also reported in Table 1.

Finally, we report in Figure 6 the results for the weak-coupling case $\Gamma = 1$. Rescaling of $b_{12}^{PY}(z)$ is now immaterial, within the accuracy of the simulation data, but curvature effects in the Poisson equation are still clearly visible.

5. Summary and discussion

We have presented above a detailed analysis of the available simulation data on the hard wall-plasma interface, as far as the current status of liquid structure theory will allow. This analysis has demonstrated, first of all, the crucial importance of embodying the contact theorem in the theory of this interface. We stress that this remains true even if one does not have an accurate description of all the other details of the density profile. Indeed, we have seen in Table 1 that even a rough description of the profile, provided it embodies correctly some bulk properties and the contact theorem, gives a satisfactory account of an important macroscopic property of the interface, namely the total potential drop at zero wall charge.

Another result of our analysis has been to indicate that curvature corrections, or more generally finiteness effects, are still quantitatively important in simulation samples as large as those already examined for the hard wall-plasma interface. Great care is clearly needed in assessing the quantitative merits of an approximate theory in such situations, and further theoretical efforts on curvature effects seem called for.

Returning, in conclusion, to the role of the contact theorem, it seems clear that a self-consistent account of the ionic densities near contact will also be important in more realistic models of electrode-electrolyte interfaces. These densities clearly provide a crucial link between the charging of the electrode and its screening by the electrolyte.

Acknowledgements. This work was supported by the Ministero della Pubblica Istruzione and by the Consiglio Nazionale delle Ricerche. The authors wish to thank Dr H.E. DeWitt for providing a tabulation of simulation data on the structure of the bulk plasma.

References

1. See e.g. 'Electrochemistry', Specialist Periodical Reports (The Chemical Society, London).
2. J.P. Badiali, M.L. Rosinberg, D. Levesque and J.J. Weis, J. Phys. C16, 2183 (1983).
3. P. Ballone, G. Senatore and M.P. Tosi, Lett. N. Cimento 31, 619 (1981).
4. D. Henderson and L. Blum, J. Chem. Phys. 69, 5441 (1978); D. Henderson, L. Blum and J.L. Lebowitz, J. Electroanal. Chem. 102, 315 (1979); D. Henderson and L. Blum, J. Chem. Phys. 75, 2025 (1981).
5. N. Totsuji, J. Chem. Phys. 75, 871 (1981).
6. See also P. Chocuard, P. Favre and C. Gruber, J. Stat. Phys. 23, 405 (1980).
7. F. Lado, Phys. Rev. A8, 2548 (1973) and Phys. Lett. 89A, 196 (1982).
8. Y. Rosenfeld and N.W. Ashcroft, Phys. Rev. A20, 1208 (1979).
9. I.K. Snook and D. Henderson, J. Chem. Phys. 68, 2134 (1978); I.K. Snook and W. van Megen, J. Chem. Phys. 70, 3099 (1979).
10. W.L. Slattery, G.D. Doolen and H.E. DeWitt, Phys. Rev. A21, 2087 (1980).
11. J.P. Hansen, Phys. Rev. A8, 3096 (1973).
12. See e.g. S.L. Carnie, D.Y.C. Chan, D.J. Mitchell and B.W. Ninham, J. Chem. Phys. 74, 1472 (1981).
13. J.L. Lebowitz, Phys. Rev. 133, A895 (1964).
14. A.D. Graves, J. Electroanal. Chem. 25, 349 and 357 (1970); K.R. Painter, P. Ballone, M.P. Tosi, P.J. Grout and N.H. March, Surface Sci. 131, 000 (1983).

Table 1. Contact density $n(0)/n$ and potential drop $\Delta\varphi$ at various coupling strengths

Γ	$n(0)/n$						$\beta e\Delta\varphi$					
	MC[a]	HNC/MC[a]	MSA/MSA[a]	MHNC/MHNC flat wall	MHNC/MHNC curved wall	Asymptotic formula	MC[a]	HNC/MC[a]	MSA/MSA[a]	MHNC/MHNC flat wall	MHNC/MHNC curved wall	Asymptotic formula
1	0.85	0.909	0.95	0.86	0.87	0.86	0.04	0.043	0.011	0.06	0.07	0.047
10	0.20	0.344	0.025	0.23	0.24	0.24	1.86	1.154	1.402	1.90	1.93	1.91
30	0.01	0.037	-1.603	0.01	0.01	0.00	7.48	4.74	7.76	7.49	7.49	7.48
70	-	-	-4.064	0.00	0.00	0.01	19.28[b]	12.59[b]	25.59	19.28	19.28	19.29

(a) From Badiali et al., Ref. 2.

(b) Values determined by assuming $n(0) = 0$.

Figure 1. Bridge function b(z) for the interface (full lines) and for the bulk (dashes), at the indicated values of the packing fraction η.

Figure 2. Interfacial density profile at $\Gamma = 30$ in the MHNC (full line) and in the HNC/MHNC (dashes) for a planar wall. The circles are simulation data by Badiali et al[2] for the plasma in a spherical cavity of radius R = 8.79 a. The appropriate values of the packing fractions in the MHNC are $\eta = 0.32$ for the bulk and $\eta' = 0.28$ for the interface.

Figure 3. Interfacial density profile at $\Gamma = 10$ in the MHNC for a flat wall (dash-dots, $\eta = 0.22$ and $\eta' = 0.17$) and for a curved wall before (dashes, $\eta' = 0.17$) and after (full line, $\eta' = 0.19$) rescaling the width of the interfacial bridge function. The circles are simulation data by Badiali et al[2] for the plasma in a spherical cavity of radius R = 8.79 a.

Figure 4. Interfacial density profile at $\Gamma = 30$ in the MHNC for a flat wall (dash-dots, $\eta = 0.32$ and $\eta' = 0.28$) and a curved wall before (dashes, $\eta' = 0.255$) and after (full line, $\eta' = 0.27$) rescaling the width of the interfacial bridge function. The circles are simulation data by Badiali et al[2] for the plasma in a spherical cavity of radius R = 8.79 a.

Figure 5. Interfacial density profile at $\Gamma = 70$ in the MHNC for a flat wall (dash-dots, $\eta = 0.395$ and $\eta' = 0.34$) and a curved wall before (dashes, $\eta' = 0.35$) and after (full line, $\eta' = 0.365$) rescaling the width of the interfacial bridge function. The circles are simulation data by Badiali et al[2] for the plasma in a spherical cavity of radius R = 6.90 a.

Figure 6. Interfacial density profile at $\Gamma = 1$ in the HNC/MHNC (dashes) and in the MHNC (full line), with inclusion of curvature effects. The circles are simulation data by Badiali et al[2] for the plasma in a spherical cavity of radius R = 6.90 a.

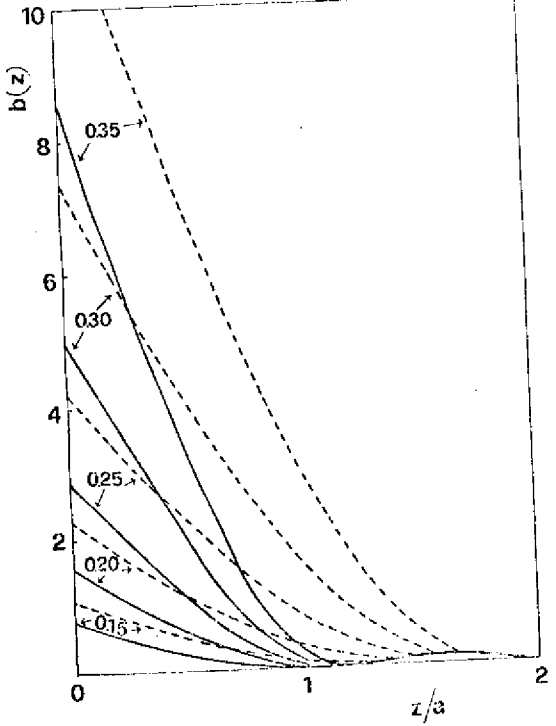

Fig.1

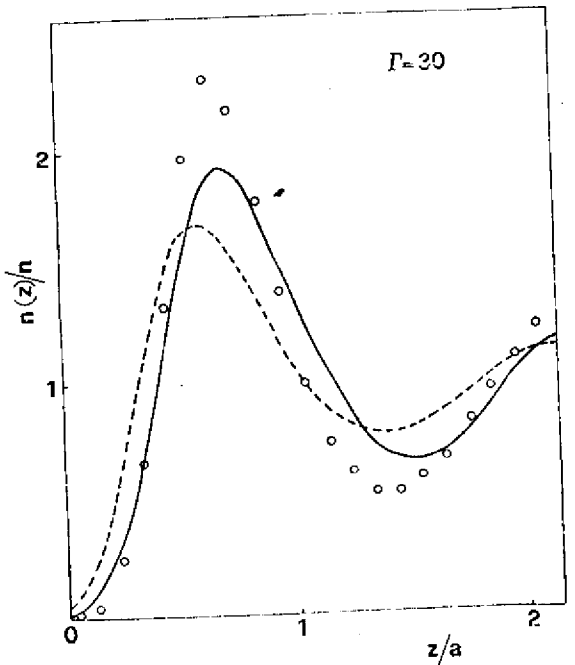

Fig.2

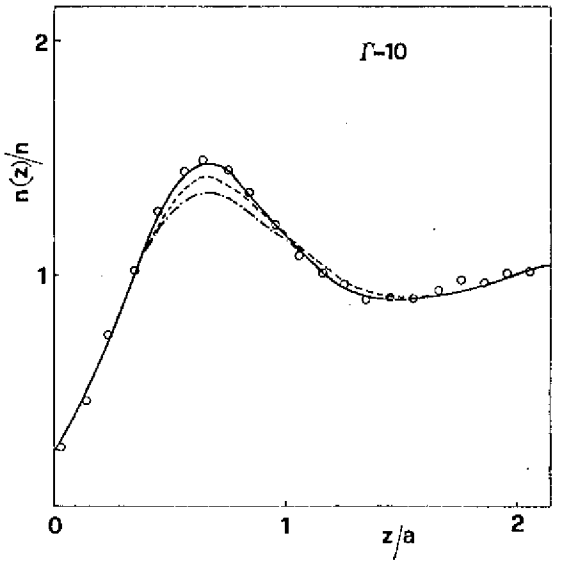

Fig.3

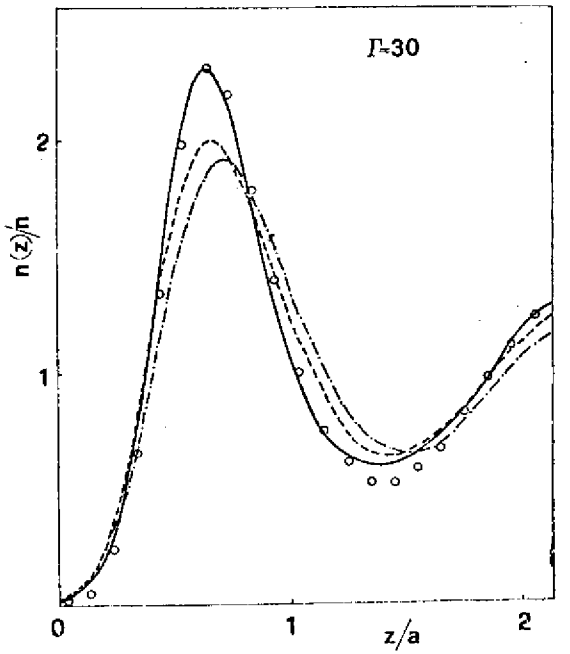

Fig.4

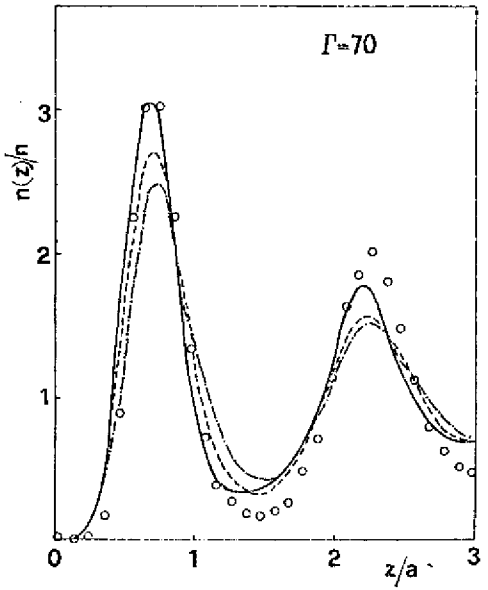

Fig.5

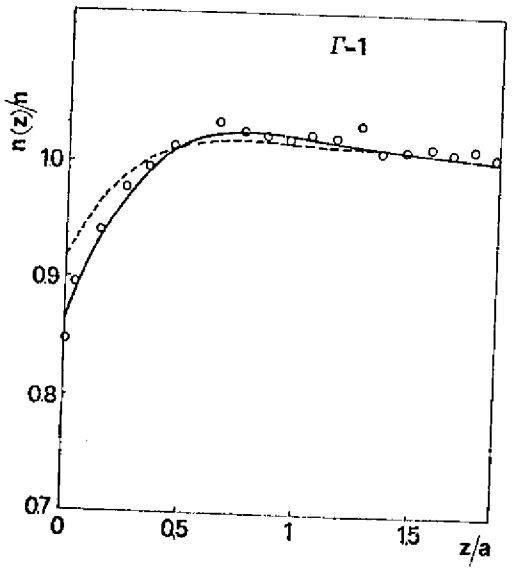

Fig.6